"A Cochlear Nucleus Auditory prosthesis based on microstimulation"

Contract No. **No. NO1-DC-4-0005**

Progress Report #4

HUNTINGTON MEDICAL RESEARCH INSTITUTES

NEURAL ENGINEERING LABORATORY

734 Fairmount Avenue

Pasadena, California 91105

D.B. McCreery, Ph.D.

L.A. Bullara, B.S.

A.S. Lossinsky, Ph.D.

HOUSE EAR INSTITUTE

2100 WEST THIRD STREET

Los Angeles, California 90057

R.V. Shannon Ph.D

S. Otto M.S.

M. Waring, Ph.D

ABSTRACT

One of the goals of this project is to develop arrays of multisite silicon substrate electrodes, which should allow placement of many more microstimulating sites within the human cochlear nucleus than is possible with discrete iridium microelectrodes. We are developing arrays for implantation into the human cochlear nucleus that have 16 electrode sites distributed on 4 silicon shanks extending from an epoxy superstructure that is 2.4 mm in diameter. We have begun to evaluate the capacity of our intranuclear microstimulating arrays to access separate neuronal population in the feline cochlear nucleus, using multi-channel, multi-unit recording of neuronal activity in the central nucleus of the inferior colliculus (ICC). Multiunit neuronal activity is recorded in the contralateral inferior colliculus using a 32-site silicon substrate probe. Neuronal activity was recorded simultaneously from 16 probe sites using custom hardware and computer software. We generated post-stimulus time (PST) histograms of the neuronal activity that was recorded at each of the 16 sites in the ICC. Contour ("topographic style") maps of the evoked neuronal activity were generated from the set of 16 PST histograms.

To date, these experiments have been directed towards perfecting our techniques and procedures prior to studies using cats with the chronically-implanted microstimulating arrays. However, we have demonstrated that the method will show when different microstimulating sites in the ventral cochlear nucleus (VCN)) are stimulating neurons in different portions of the tonotopic gradient in the VCN, even when the stimulus amplitude was sufficiently high such that there was bound to be considerable overlap of the neuronal populations activated from adjacent stimulating sites. The shanks of the microstimulating array penetrated into the cochlear nucleus from its dorsolateral surface, and the degree to which adjacent microstimulating sites could access the neuronal population subserving differed acoustic frequencies differed significantly for shanks that penetrated into different regions of the nucleus. Overall,

our findings are consistent with neuroanatomical studies of the tonotopic organization of the feline ventral cochlear nucleus. Our approach will allow us to evaluate various spacings between the simulating sites on individual shanks of our silicon-substrate arrays, and the effects of various spacings between different shanks, and different sites of penetration of the shanks into the cochlear nucleus.

To date, five patient have been implanted with arrays of 14 macroelectrodes on the surface of their cochlear nucleus and 8 penetrating microelectrodes into or near their ventral cochlear nucleus, the penetrating auditory brainstem implant or "PABI". All were afflicted with type II neurofibromatosis and with bilateral acoustic schwannomas and the electrode arrays were implanted after remove of the second tumor. PABI patients continue to show low levels of open set sentence recognition, even after more than one year of daily experience. One potential problem identified is the 3 nC charge limit. For PABI patients who receive hearing on the penetrating electrodes, few receive loud sensations at the 3 nC level, so speech processor programs that use penetrating electrodes do not produce loud sensations on those electrodes, resulting in limited utility of the penetrating electrodes in real-world listening conditions. The next generation of penetrating electrodes will utilize a larger surface area and higher charge limit to overcome these possible limitations.

1: Development of a multi-site silicon-substrate electrode array

INTRODUCTION

The workscope of our contract calls for the development of arrays of silicon substrate electrodes, which should allow placement of many more electrode sites into the human cochlear nucleus than is possible with discrete iridium microelectrodes. We are developing arrays for implantation into the human cochlear nucleus that have 16 electrode sites distributed on 4 silicon shanks extending from an epoxy superstructure that is 2.4 mm in diameter. This is the same footprint as our first-generation human arrays employing discrete iridium microelectrodes and is designed to be implanted using the same inserter tool.

We have been conducting animal studies using microstimulating arrays with silicon substrate probes fabricated at the University of Michigan under the direction of Design Engineer Jamille Hetke. Figure 1-1A shows a probe with 2 shanks and 8 stimulating sites, that have been sputter-coated with iridium oxide. The 4 sites on each shank are located between 0.8 to 1.7 mm below the top of the shanks. Figure 1-1B shows an array with 2 of the probes (4 shanks and 16 electrode sites) extending from an epoxy superstructure that floats of the surface of the cochlear nucleus. The cable is angled vertically, to accommodate the trans-cerebellar approach to the feline cochlear nucleus.

In principle, the silicon substrate array could provide improve functionality of a central auditory prosthesis by affording highly localized stimulation of neuronal populations within the ventral cochlear nucleus (VCN). One facet of this capacity for localized stimulation is the ability to access the tonotopic organization within each of the subdivisions of the cochlear nucleus (CN). In previous reports, we have described a method of quantifying this capability in chronically-implanted intranuclear silicon arrays using current source-sink density analysis in the contralateral inferior colliculus. The tonotopic organization of the anteroventral and posteroventral CN is preserved in the projection from the CN to the inferior colliculus as illustrated schematically in figure 1-2. The projection is primarily to the contralateral colliculus. The iso-frequency

laminae are oriented more- or- less perpendicular to the dorsolateral-venteromedial axis of the central nucleus of the inferior colliculus (ICC) with lower acoustic frequencies represented dorsally and high frequencies represented ventrally and medially (e.g. Semple and Aitkins, 1979) In this report, we described our first experiences with an approach based on simultaneous recording of individual neuronal action potentials in the ICC. Since individual neuronal action potentials (spikes) can be recorded only from neuronal cell bodies or axons that are within a few hundreds of microns of the recording site, the approach should allow improved definition of the spatial pattern of neuronal activity in the ICC.

METHODS

To date, we have conducted 2 animal experiments using microstimulation arrays implanted acutely in the cochlear nucleus. These experiments were conducted in order to perfect our techniques and procedures prior to the studies that will use the cats with the chronically-implanted microstimulating arrays. The microstimulating arrays used in the 2 acute experiments had manufacturing defects and only a few usable sites, but they were adequate to accomplish the goals of this study.

The 2 adult cats were anesthetized with Isoflurane and nitrous oxide, their heads fixed in a stereotaxic holder, and a wide craniectomy was made over the left posterior cerebral hemisphere. The occipital pole of the cerebrum was removed by aspiration to expose the inferior colliculus. In one cat, most of the colliculus was caudal of the rostral edge of the boney tentorium, and a portion of the tentorium was resected to expose the IC. A second craniectomy was made over the right cerebellum, and the lateral cerebellum was aspirated to expose the dorsolateral surface of the right cochlear nucleus. The microstimulating array was inserted into the dorsolateral surface of the nucleus at an angle of about 40˚ from the vertical so that the underside of the array's superstructure would lie flat on the sloping dorsolateral surface of the CN, as is done when the arrays are implanted chronically. The cats were then transported to a double-walled acoustic isolation room with their heads still fixed in the stereotaxic

holder. Throughout the remainder of the experiment, anesthesia was maintained with a mixture of 2-2.5% Isoflurane and oxygen delivered by a self-breathing apparatus. Their respiration rate and end-tidal CO_2 was monitored continuously. Core body temperature was maintained at 37.5-39.0°C using a circulating water heating pad. All sound-generating equipment was located outside of the sound isolation room.

Multiunit neuronal activity is recorded in the contralateral inferior colliculus using a 32-site silicon substrate probe (Figure 1-3) designed and fabricated by NeuroNexus, Inc., and kindly provided by Dr. Russell Snyder. The recording sites are spaced 100 µm apart over a total span of 3.1 mm, which is somewhat less than the width of the domestic cat's ICC along the dorsolateral-ventromedial axis (approximately 4.5 mm). (A probe spanning 4.5 mm is presently under development at HMRI). The recording array was inserted into the inferior colliculus at an angle of 45° from the vertical, and approximately along the tonotopic gradient. Initially, the probe was inserted to a depth such that the uppermost recording site was 1 mm below the surface of the colliculus; approximately at the dorsolateral margin of the central nucleus. After data collection, the probe was advanced by 1 mm so as to place the deepest site near the ventromedial margin of the nucleus. Neuronal activity was recorded simultaneously from alternate probe sites (16 sites) using the custom hardware and computer software described in previous progress reports. Neuronal action potentials ("spikes") with very good signal-to-noise ratios (>20× the RMS noise level) were often recorded from 1 to 3 of the sites in the ICC, but most of the spikes were of low amplitude with signal-to-noise ratios of 5 or less. As shown in Figure 1-4, trace A, repetitive pulsatile microstimulation in the contralateral ventral cochlear nucleus induces a large compound evoked response in the contralateral ICC, which typically is much larger than the superimposed spikes. Also, the frequency spectra of the spikes and evoked response partially overlap so that spikes and the evoked response cannot be fully separated by conventional band-pass filtering. Therefore, we have adapted a technique often used in image processing, which usually is described as "common element subtraction" or "common background suppression". First, a common template is generated by summing (averaging) 1500 successive responses to the

microstimulation (Figure 1-4, Trace B). This template then is subtracted from each individual trace (response) . Low- and high-frequency noise that is unique to each trace then is removed by broadband filtering using a passband of 1000-8000 Hz (time domain convolution filter using sinx/x kernels). Figure 1-5C shows an individual post-stimulus trace after this processing. This trace did not contain resolvable spikes. The large evoked response is well suppressed, allowing spikes to be detected with a conventional windowing discriminator; in this study, we have set the spike discrimination threshold at 3.5 × the rMS noise level. Traces with spikes at various post-stimulus latencies are shown in Figure 1-4, Traces D, E & F. The common element suppression procedure is applicable only when spikes are not tightly time-locked to the stimulus, since these become part of the common template and thus are removed from the individual traces. The software does includes a provision to extrapolate between two points on either side of the signature of these time-locked spikes so that their signature is deleted from the template, allowing the spikes to appear in the individual traces. However, in our study, it is the activity of the output neurons from the ICC that is of primary interest. Their (postsynaptically-induced) activity is more dispersed temporally, and we have not found it to be necessary to use the extrapolation feature.

Controlled-current, biphasic stimulus pulses (150 μs/ph in duration at 50 Hz) were applied to the individual microelectrode sites in the cochlear nucleus. Most of the data were acquired using a stimulus amplitude of 30 μA (4.5 nC/ph). This is the maximum charge per phase used in previous studies to generate the response growth functions that are used to characterize the long-term stability of the chronically implanted electrodes in the cat cochlear nucleus. In the human patients implanted to date, the thresholds for auditory percepts from the penetrating microelectrodes have been 1.7 nC/phase or below.

The response to 1,500 successive stimulus pulses delivered to each microstimulating site was recorded simultaneously from 16 sites in the contralateral ICC. In the second cat, the response to acoustic stimuli also was recorded in the ICC for each penetration of the recording probe. Tone bursts of 1.0, 2.5, 4.5, and 7.5 KHz

(approximately 85 db spl) and 100 ms in duration with a rise time of 10 ms were used. In the future, we plan to replace our loudspeaker with a unit with improved high-frequency response so that we can include the responses to tones about 10 KHz, which are represented in the venteromedial part of the ICC.

We generated post-stimulus time (pST) histograms of the neuronal activity that was recorded at each of the 16 sites in the ICC. Figure 1-5 depicts the location of the microstimulating sites on the microelectrode array in the cochlear nucleus of cat CN156 (The rostral-medial shank had fractured and detached during fabrication). Figure 1-6 shows a pST histogram evoked from site 3 in the CN and recorded from site 8 in the contralateral ICC. Contour ("topographic style") maps of the evoked neuronal activity were generated from the set of 16 PST histograms. Figures 1-7A,B,C show the contour maps of neuronal activity evoked from sites 3,10 and 14 on the caudal-lateral shank of the stimulating electrode, in the posteroventral cochlear nucleus (PVCN). On these contour maps, the ordinant is the distance above the deepest recording site in the ICC (at the tip of the probe), and the abscissa is time after the stimulus pulse. The contour line labels represent the total number of action potentials in each of the 100 μs bins of the PST histograms from which the maps were constructed. The maxima of the response to the acoustic tones of different frequencies is indicated near the y-axis. In these maps, the neuronal activity evoked from each stimulating site in the CN is distributed over a range of depths in the ICC. The post-stimulus latency of the response maxima is approximately the same at each depth in the ICC, with the maxima of the shallow activity occurring an average of 100 to 200 μs earlier than maxima of the deepest activity. Thus this distribution of activity over depth in the ICC may represent neuronal activity recorded from axons projecting out of the central nucleus. If this is the case, the shallowest activity represents the neurons activated by the microstimulation in the CN. In Figure 1-7, the maxima of neuronal activity evoked from sites 3,10 and 14 occur at progressively shallower depths in the ICC, spanning the range of about 7.5 to slightly above 4 kHz.. This ordering is as expected, since site 3 was shallowest in the PVCN, and site 14 was deepest.

Figures 1-8 A,B,C show the neuronal activity evoked from sites 7,11,15 on the caudal-medial shank in the CN of cat CN156. This shank also was in the caudal part of the CN, but more medial than the shank depicted in figure 1-7 (see figure 1-5). In this case, the response maxima show greater separation in the ICC than in figure 1-7. Here also the maxima of the neuronal activity evoked from the more ventral sites in the CN are shallower in the ICC. Also, the activity evoked from the caudal-medial shank (Figure 1-8) is deeper in the ICC (in the region of higher acoustic frequencies) than the activity evoked from the caudal-lateral shank (Figure 1-7). This also is as expected, since a probe shank penetrating from the dorsolateral surface of the CN will travers the isofrequency laminae at an angle, with the more medial shank intersecting higher frequency laminae, as depicted in figure 1-10.

Figure 1-9 shows the responses evoked in the ICC from electrode sites 8,12 and 16 on the rostral-lateral shank of the array of the same cat (CN156). Based on its site of penetration into the CN, this shank was in the medial part of the anteroventral cochlear nucleus. Here, the maxima of the neuronal responses in the ICC was deep to the 7.5 kHz point and the maximum of the responses from all three stimulating sites in the CN was at the same depth in the ICC. As discussed below, this is not unexpected for a probe entering the AVCN from the dorsolateral surface of the CN.

DISCUSSION

We have begun to evaluate the capacity of our intranuclear microstimulating arrays to access separate neuronal population in the feline cochlear nucleus, using multi-channel, multi-unit recording in the central nucleus of the inferior colliculus. To date, these experiments have been directed towards perfecting our techniques and procedures prior to studies using cats with the chronically-implanted microstimulating arrays. However, we have demonstrated that the method will show when different microstimulating sites are stimulating neurons in different portions of the tonotopic gradients in the ventral cochlear nucleus, even when the stimulus amplitude was sufficiently high such that there was bound to be considerable overlap of the neuronal populations activated from adjacent stimulating sites. This technique will allow us to

evaluate various spacings between the simulating sites on individual shanks of our silicon-substrate arrays, and the effects of various spacings between different shanks, and for different sites of penetration of the shanks into the cochlear nucleus.

Our findings are consistent with neuroanatomical studies of the tonotopic organization of the feline ventral cochlear nucleus. Snyder et al (1997) examined the tonotopic organization of the primary afferent projections to the cochlear nucleus in adults cats, using focal extracellular injections of Neurobiotin (NB) into the spiral ganglion of the basal cochlea. One to three injections were made along the basal one-third of the cochlea. Each injection produced discrete laminae of labeled afferent axon terminal that correspond to the a narrow band of acoustic frequencies ("isofrequency laminae"). These were distributed in a dorsal- to- ventral sequence, across each major CN subdivision: the anteroventral, posteroventral, and dorsal cochlear nucleus. Figure 1-10 shows two illustrations from their study, with superimposed sketches of an electrode array inserted into the dorsolateral surface of the nucleus. The Neurobiotin labeling representing the isofrequency lamina are shown as dark bands. In our cats the microstimulating arrays are inserted into the dorsolateral surface of the ventral cochlear nucleus, as depicted in the superimposed sketches. In the caudal part of the VCN, in the PVCN (Figure 1-10A), the isofrequency laminae are nearly planar and are inclined with respect to the dorsolateral surface of the nucleus. Thus a silicon shank penetrating from the dorsolateral surface of the nucleus would be expected to traverse a portion of the tonotopic gradient, and stimulating sites close to the superstructure of the array would be expected to excite high-frequency neurons in the PVCN which project to sites deep in the IC (and vice- versa for sites near the tips of the probe). This is what is shown in figures 1-7 and 1-8. However, because the shanks cross the tonotopic strata obliquely, more than one probe will be required to gain access to the entire tonotopic gradient of the PVCN, as exemplified by a comparison of Figure 1-7 and 1-8. In humans, the microstimulating electrodes are most likely to penetrate into the PVCN, since the AVCN is partly hidden beneath the middle cerebellar peduncle. More rostrally, in the feline AVCN, the isofrequency laminae also are ordered, with the high acoustic frequencies represented dorsally and low frequencies ventrally but the

laminae tend to be oriented nearly perpendicular to the dorsolateral surface of the nucleus, or to be somewhat cup-shaped (Figure 1-10B). The tonotopic ordering of the response from stimulating sites distributed along a probe inserted into this region from the dorsal-lateral surface of the CN would be less predictable, and only a small portion of the tonotopic gradient might be accessed by any one probe. Thus In figure 1-9, all three stimulating sites on the shank in the AVCN of cat CN156 appear to excite the same part of the tonotopic gradient.

In our maps of evoked multi-unit neuronal activity vs depth in the ICC, the activity evoked from each stimulating site in the CN is distributed over a range of depths in the ICC, with nearly identical latency of the response maxima at all depths in the ICC. This distribution of activity over depth in the ICC may represent neuronal activity recorded from axons projecting out of the central nucleus, rather than an extended distribution of synaptic activity across depth, which would indicate that the intranuclear microstimulation is activating neurons representing a wide range of acoustic frequencies. Previously, we have used current sink-source analysis to localize neuronal activity induced in the ICC by intranuclear microstimulation (McCreery et al, 1998). Current sources are generally equated with regions of excitatory synaptic activity, and our maps of sources and sink in the ICC have shown these to be confined to a narrow range of depths. In principle, source-sink analysis can be performed using set of the averaged templates extracted from the same recordings used for the multi-unit studies (See figure 1-4). However, this will require very precise calibration of each recording channel, and for each recording probe, across the frequency spectrum of the compound evoked response. This task will be included in the work for next quarter.

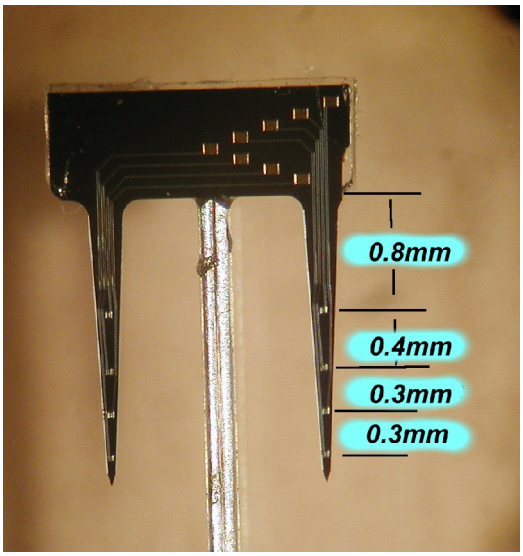

Figure 1-1A

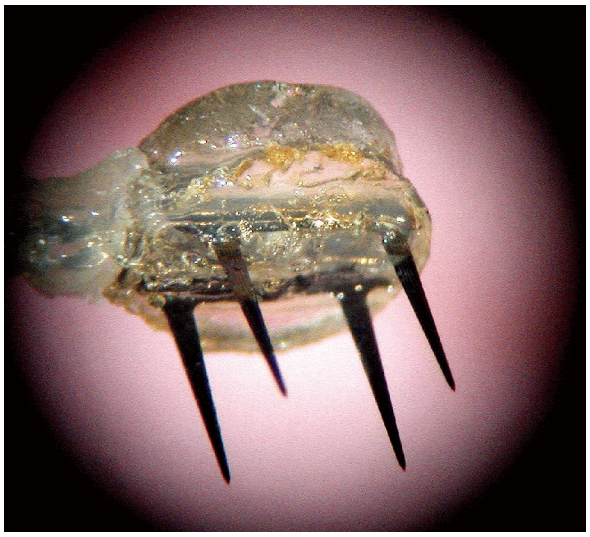
Figure 1-1B

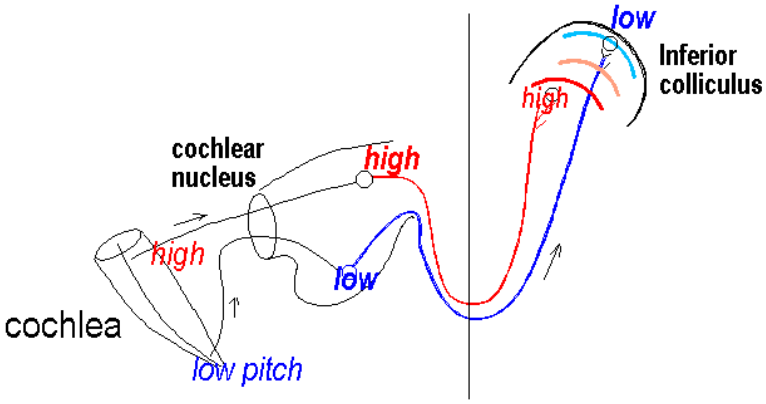

Figure 1-2

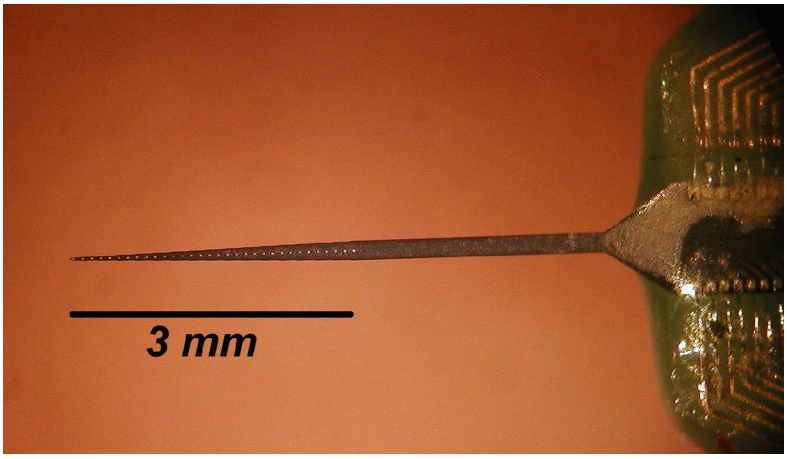

Figure 1-3

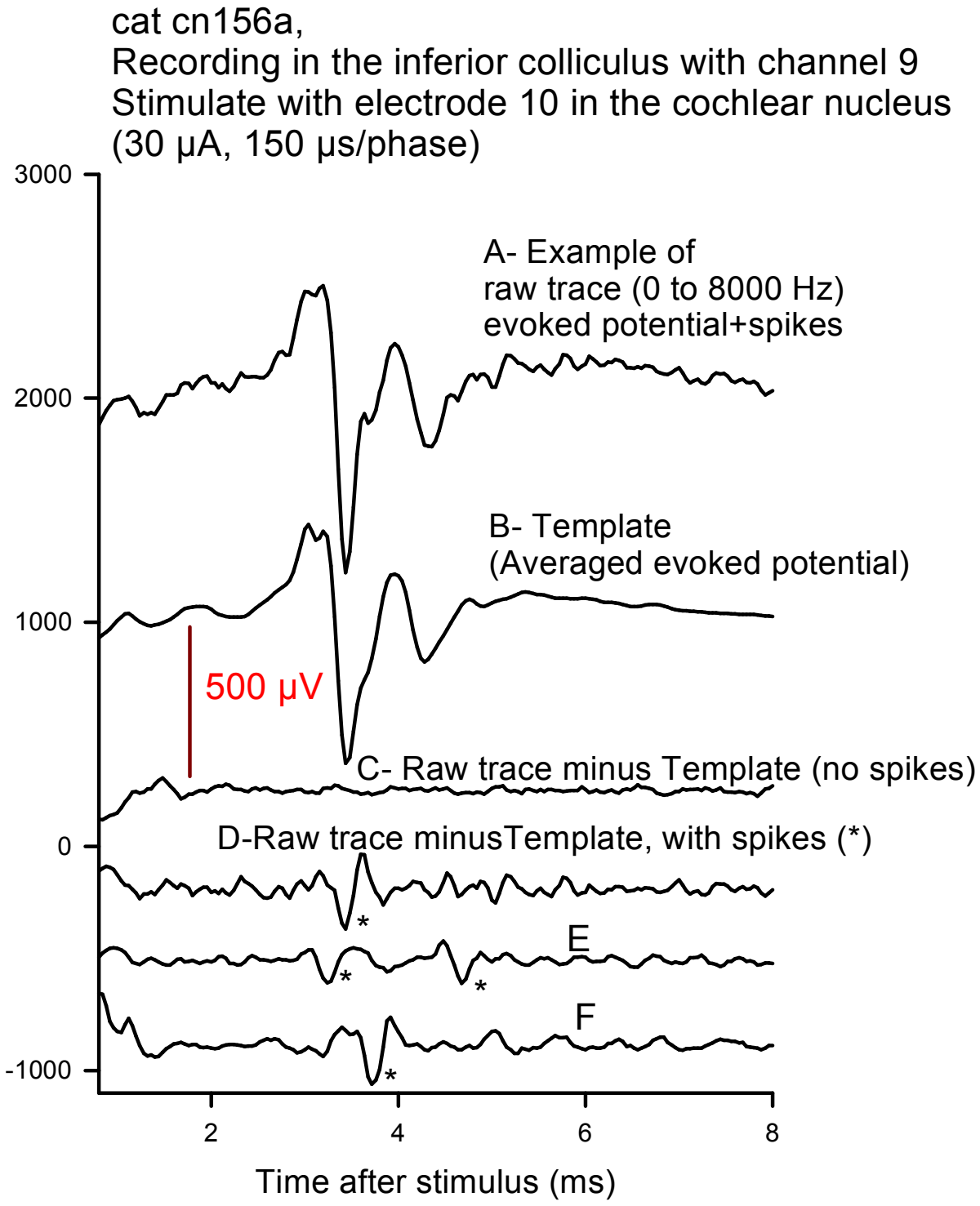
cat cn156a,
Recording in the inferior colliculus with channel 9
Stimulate with electrode 10 in the cochlear nucleus
(30 µA, 150 µs/phase)
3000
2000
1000
0
-1000
A- Example of
raw trace (0 to 8000 Hz)
evoked potential+spikes
B- Template
(Averaged evoked potential)
500 µV
C- Raw trace minus Template (no spikes)
D-Raw trace minusTemplate, with spikes (*)
E
F
*
2
4
6
8
Time after stimulus (ms)

Figure 1-4

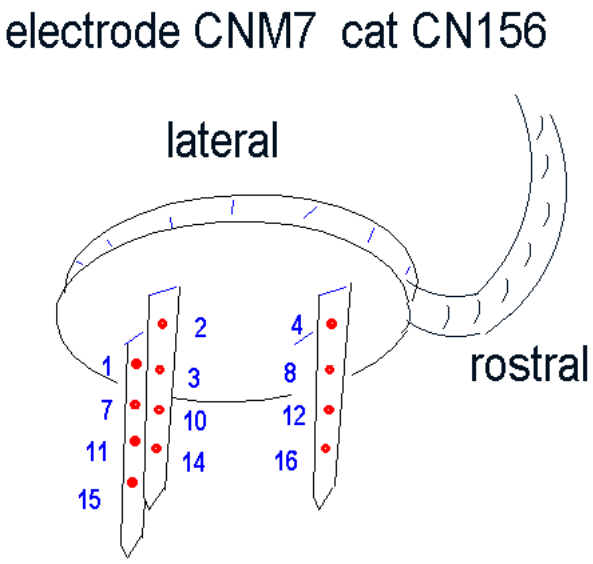

Figure 1-5

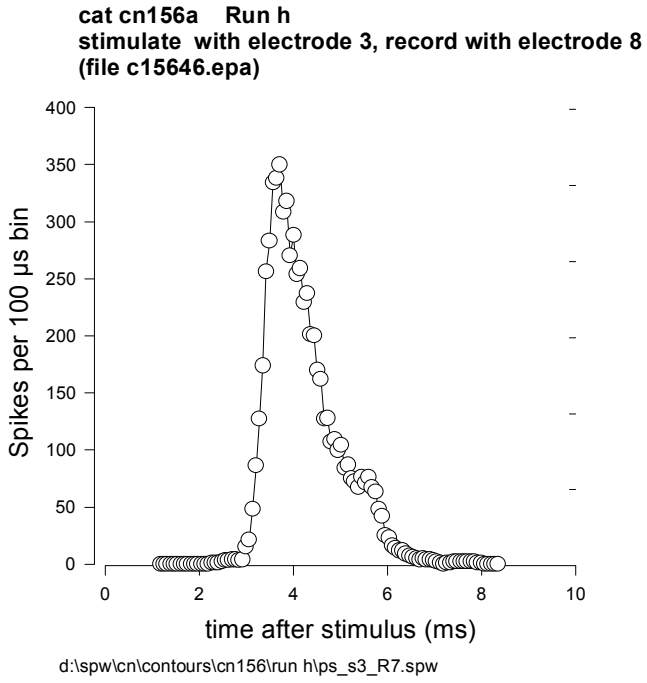

Figure 1-6

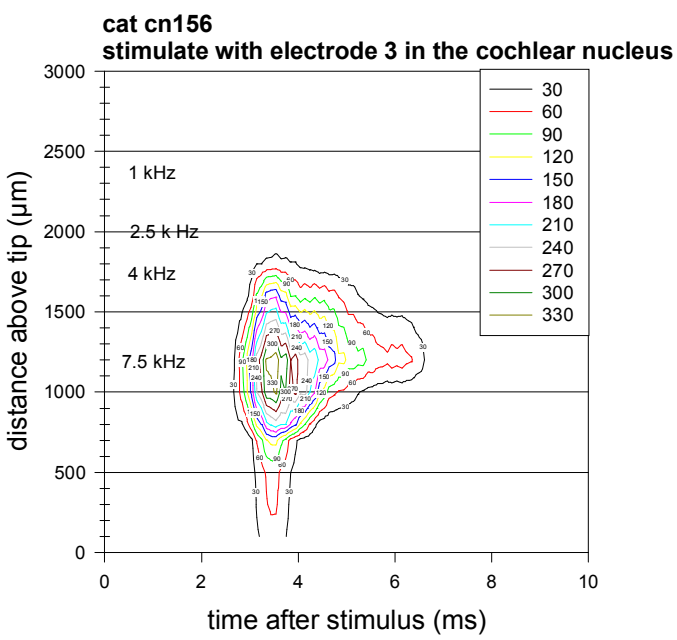

Figure 1-7A

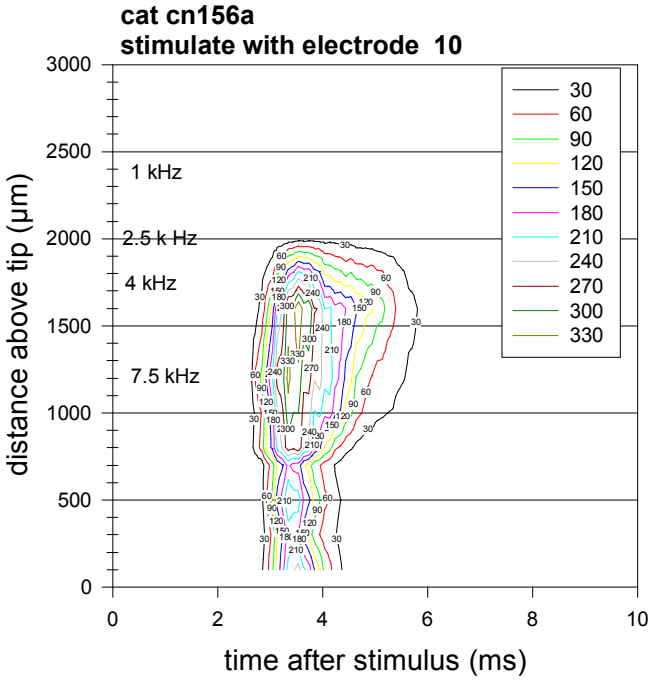

Figure 1-7B

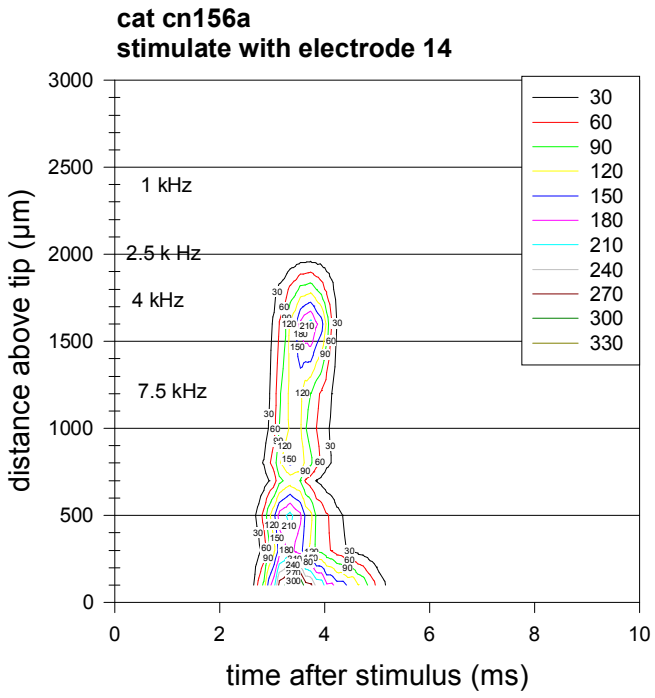

Figure 1-7C

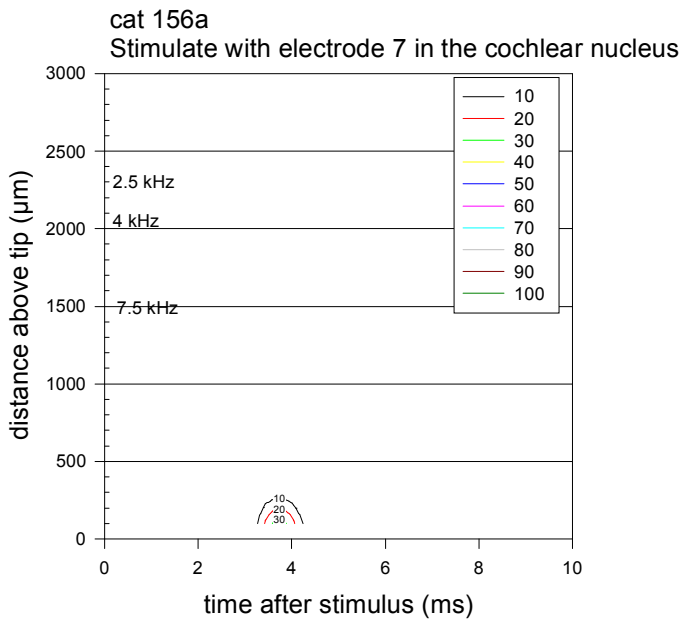

Figure 1-8A

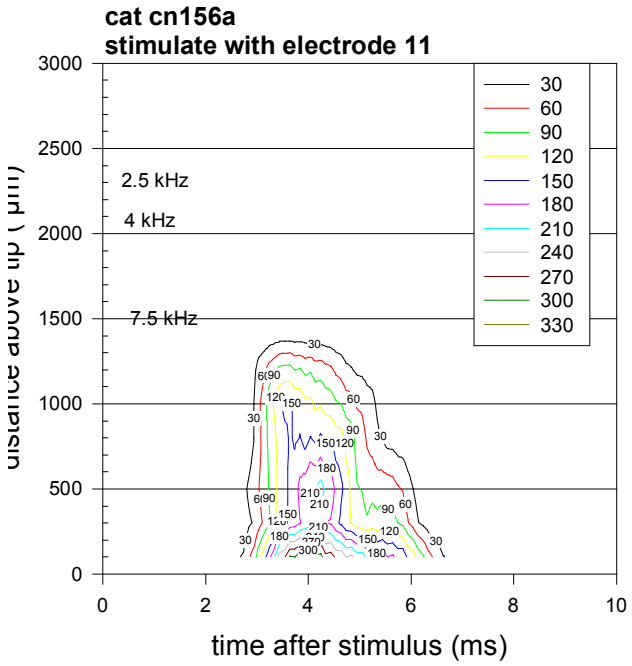

Figure 1-8B

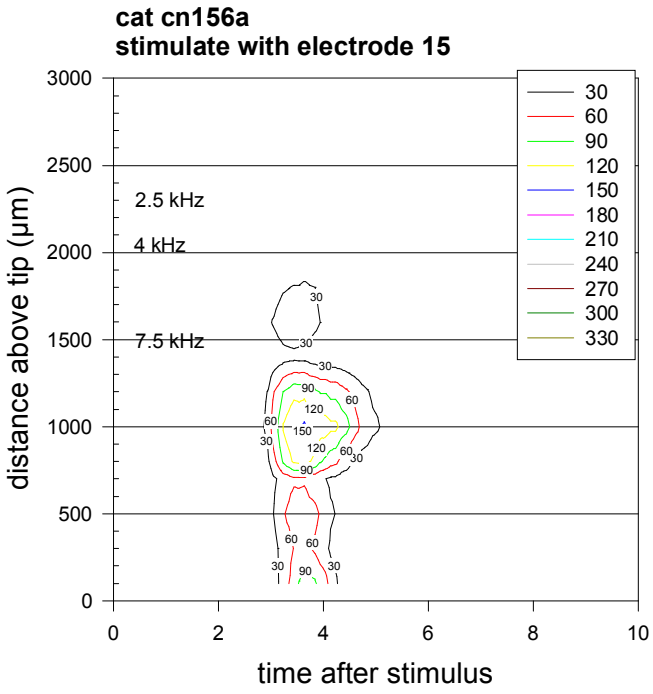

Figure 1-8C

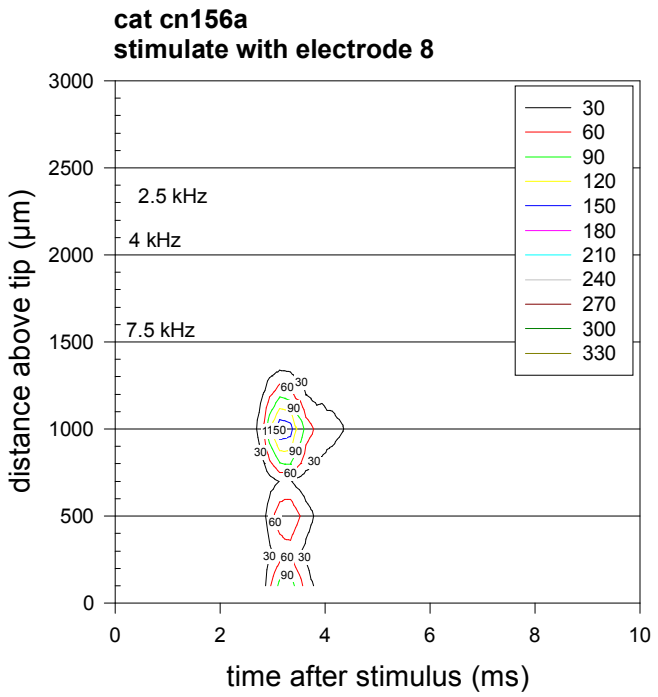

Figure 1-9A

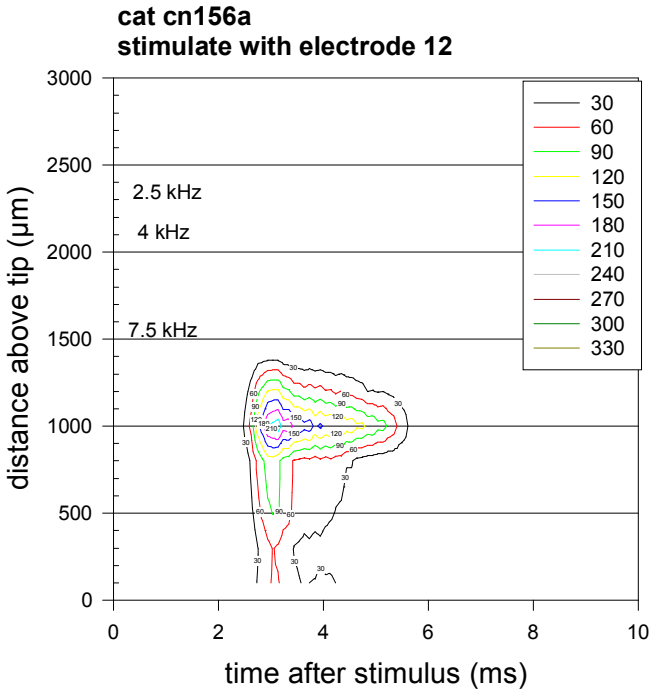

Figure 1-9B

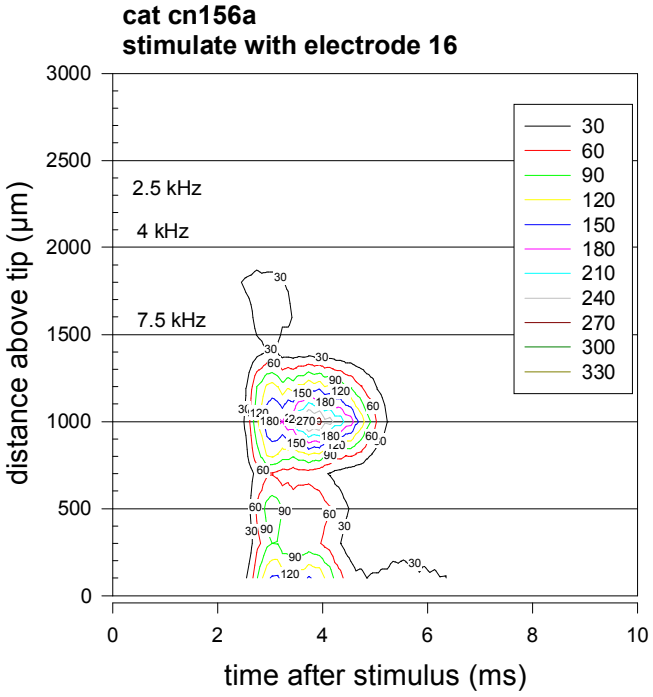

Figure 1-9C

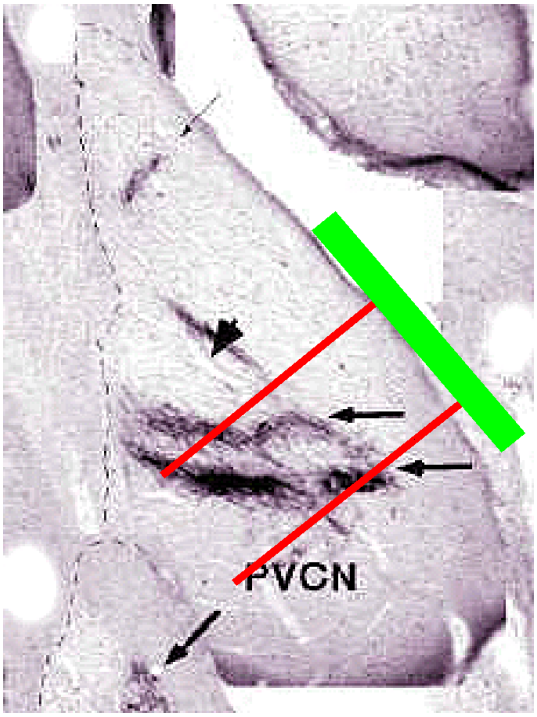

Figure 1-10A

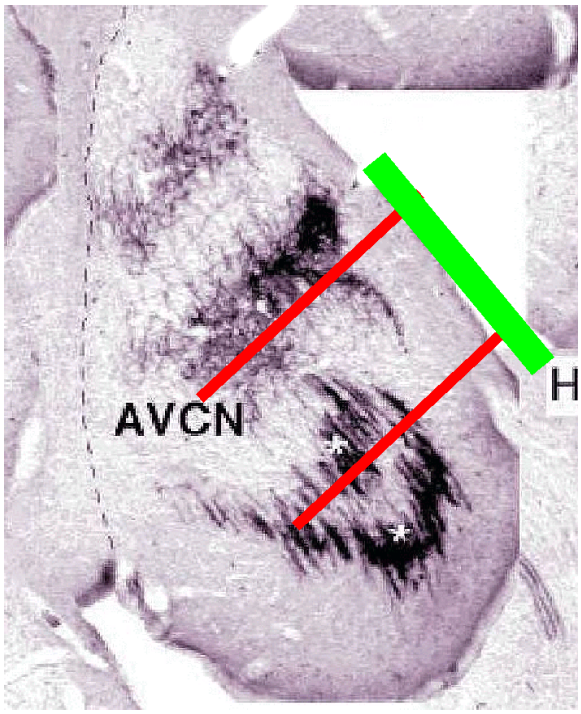

Figure 1-10B

2: Update on patients with the penetrating electrode arrays

Five patient have been implanted with arrays of 14 macroelectrodes on the surface of their cochlear nucleus and with 8 penetrating microelectrodes in or near their ventral cochlear nucleus; the penetrating auditory brainstem implant (PABI). All were afflicted with type II Neurofibromatosis and with bilateral acoustic schwannomas and the electrode arrays were implanted after remove of the second tumor.

Only one of the present five PABI patients was scheduled for follow- up testing in the second quarter of 2005. Routine clinical follow-up includes measurement of thresholds and maximum comfort levels (MCL) on each electrode, rechecking electrodes that previously produced non-auditory side effects, and adjusting the mappings on the three speech processors given each patient: surface-electrodes only map, penetrating electrodes -only map (if possible), and combination surface-penetrating map.

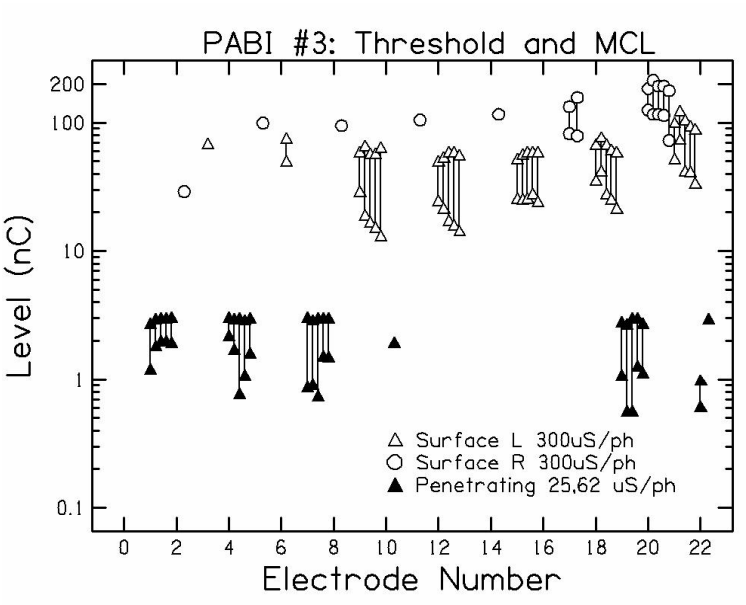

Figure 2-1

Threshold and MCL. PABI patient #3 was seen on May 6-8. Thresholds and MCLs on all electrodes were stable. Auditory sensations could be measured on 4 of the penetrating electrodes, but MCL could not be reached on any of the four at the charge limit of 3 nC. Threshold levels on surface electrodes were stable and even declined slightly on several electrodes (Figure 2-1). The most recent set of threshold-MCL measures are shown as the rightmost pair of each cluster.).

Electrode interaction.

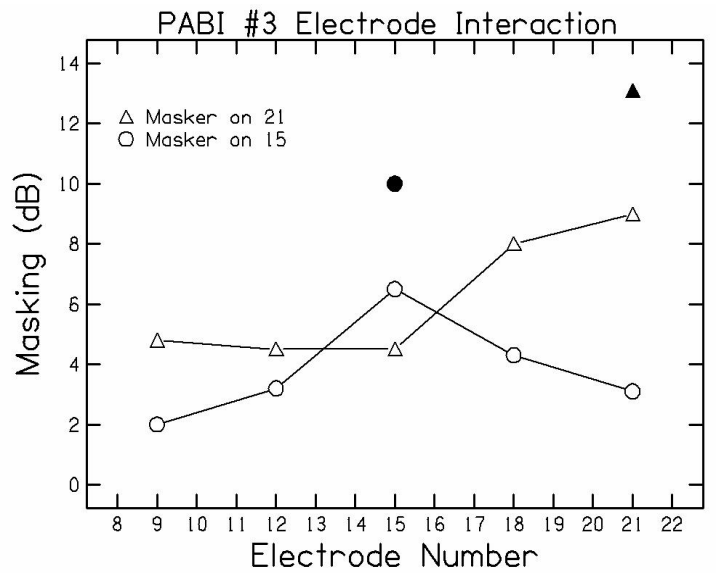

Figure 2-2

Electrode interaction was measured on PABI#3 with two methods: forward masking interference patterns and electrode discrimination. In forward masking a masker stimulus is presented for 300-400 msec on a selected electrode. A brief (20 ms) signal stimulus is presented on a different electrode 10 ms following the termination of the masking stimulus. The concept is that the residual adaptation caused by the masker will elevate the threshold of the signal. If masker and signal electrode are activating the same neural population then the amount of masking will be similar to that obtained if the masker and signal were presented to the same electrode. If masker and signal electrode are activating independent populations of neurons then the masker should not produce elevation in the threshold of the signal. The pattern of threshold increase should thus reflect the degree of overlap in neural populations stimulated by masker and signal. Figure 2-2 presents two masking patterns obtained from PABI#3. In one case the masker was presented to electrode 21 and in the other case the masker was presented to electrode 15. Both electrodes were surface electrodes located along the same side of the surface array. Both maskers were selected to produce a sound that was rated as a 6-7 in loudness on a 0-10 scale of loudness. Thresholds were measured on each electrode for 20 ms signals, which constituted a baseline level from which masking was assessed. Figure 2-2 plots the amount of masking (above the threshold level for 20 ms stimulus) as a function of electrode position. The masker electrode and level are indicated as filled symbols. The masker level is indicated in dB relative to the threshold for a 300 ms signal. Note that the maximum amount of masking was

observed when masker and signal were presented to the same electrode, as expected. The amount of masking decreased as the distance between masker and signal electrode was increased. When the masker was located on electrode 21 the amount of masking decreased as the signal was moved to electrode 18 and then 15, but the amount of masking stayed approximately constant at 4 dB for electrodes 9, 12 and 15. The surface electrodes 9-12-15-18-21 were spaced about 1 mm apart and arranged in a line along one side of the surface electrode array. We are presently working on a model of electrical fields that will allow us to estimate the spreading constant in the tissue and fluid in the vicinity of the electrode array from both threshold measures and electrode interference patterns. This model should also allow the estimation of the distance between electrode contacts and neurons.

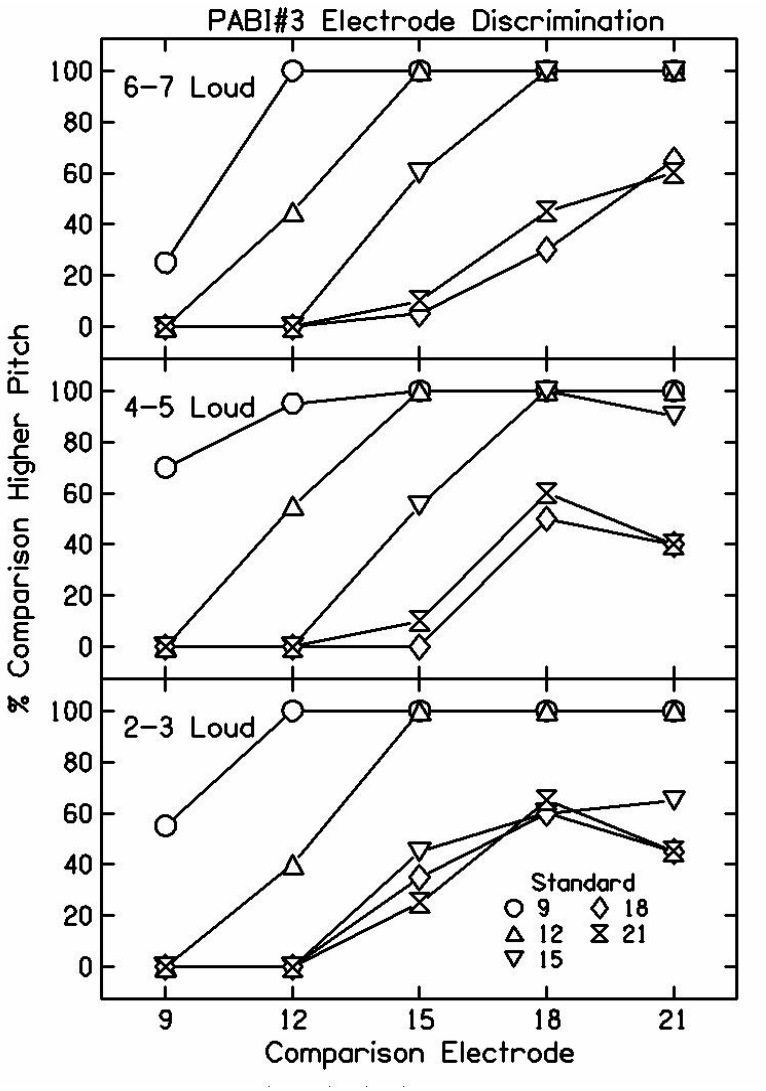

Figure 2-3

Another measure of electrode interaction is pitch discrimination. Three sets of stimuli were prepared for this test. Stimuli were presented to surface electrodes 9, 12, 15, 18, and 21 and balanced in loudness across the electrodes at three loudness levels: 2-3, 4-5, and 6-7 loudness on a 10 point loudness scale. In subjective terms these levels represent soft, comfortable, and loud sounds

respectively. For each set two electrodes were selected at random and presented to the listener. The listener was instructed to select which of the two stimuli was higher in pitch. All possible combinations and orderings of the 5 electrodes were presented 20 times each. Figure 2-3 presents the data. The top panel presents the results from the loud stimuli (6-7 loud), the middle panel presents results from the comfortably loud (4-5 loud) sounds, and the lower panel presents results from the soft (2-3 loud) stimuli. Within each panel the curves present the percent of time when the electrode on the abscissa was judged to be higher in pitch than the standard electrode. Each curve presents results from a different electrode used as the standard. One question was whether the pattern of discrimination would change substantially as a function of level. It is apparent in Figure 2-3 that the pattern changed slightly but not substantially. Electrodes were ordered in pitch in concert with their numerical value, i.e., electrode 9 was lowest in pitch, 12 was higher in pitch, and 15 was higher still. There were essentially no confusions in pitch order between electrodes 9, 12, and 15, indicating that they each produced a distinct pitch that could be reliably ranked in pitch order relative the adjacent electrodes. Electrodes 18 and 21 were reliably judged to be higher in pitch than electrodes 9 and 12. However, there was no clear difference in pitch between electrodes 18 and 21 at medium and high loudness levels, and there was no clear difference between electrodes 15, 18 and 21 at low loudness levels. This pattern of results is a bit surprising - we would expect the electrical fields from each electrode to produce broader and more overlapping patterns of excitation at loud stimulation levels and so would expect more clear pitch distinctions at low levels. Note that electrodes 18 and 21 have the highest threshold levels and so are presumably furthest from the stimulated neurons. It is possible that both electrodes are located medially to the medial edge of the cochlear nucleus and threshold level indicates the current level at which the activating current field reaches the edge of the CN. Since the same neuronal population may be stimulated by both electrodes at the medial edge of the CN, they are indistinguishable in terms of pitch.

Speech results. Data from the standard battery of speech tests were collected from PABI#3 to assess performance over time. Each PABI patient is fit with three processors for home use: all surface electrodes, all penetrating electrodes (if possible), and a combination of surface and penetrating electrodes. This patient continues to have essentially normal hearing in the contralateral ear in spite of a large (>2cm) tumor in that ear, and so only uses the PABI device for a short periods each day (plugging the TV audio directly into the PABI processor and turning the sound off on the TV). Thus, his experience with the PABI processor is limited. Figure 2-4 presents the latest speech test results of all 5 PABI patients as a function of time. Performance presented is that obtained with the best processor, which was the combination processor utilizing surface and penetrating electrodes for PABI 1-3, and surface electrodes only for PABI 4-5. PABI 4 and 5 constitute a control group in the sense that they did not obtain sound sensation on the penetrating electrodes and so are equivalent to patients with standard surface electrode ABI devices. PABI#2 continues to obtain the best speech recognition scores and on the sound-only tests there is no clear difference between the other 4 PABI listeners. PABI#2 scores similarly with the surface electrode maps and the combination maps on phoneme tests, but does clearly better on sentence recognition with the combination map, which is the map she uses most.

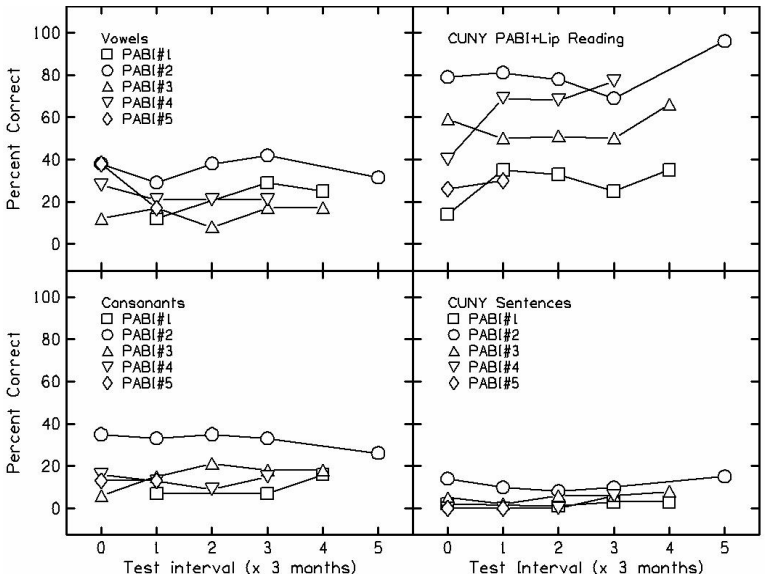

Figure 2-4

In summary, PABI patients continue to show low levels of open set sentence recognition, even after more than one year of daily experience. One potential problem identified is the 3 nC charge limit. For the PABI patients who receive

hearing on the penetrating electrodes, few receive loud sensations at the 3 nC level, so speech processor programs that use penetrating electrodes do not produce loud sensations on those electrodes, resulting in limited utility of the penetrating electrodes in real-world listening conditions. The next generation of penetrating electrodes will utilize a larger surface area and higher charge limit to overcome these limitations.

Other activities at the House Ear Institute:

Steve Otto and Bob Shannon continue to respond to inquiries from many potential PABI candidates.

Electrode redesign and patient selection issues are routinely discussed at our by-weekly ABI/PABI team meetings. The second generation of PABI electrodes is presently being fabricated by Cochlear Ltd. In Sydney Australia with an estimated delivery time of late summer-early fall 2005. A document requesting modifications of the PABI IDE were submitted to the FDA in July, requesting (1) authorization to implant an additional 10 PABI patients, (2) the addition of two additional penetrating electrodes to the array, (3) increasing the surface area of the penetrating electrodes, and (4) increasing the charge limit to 8 nC.

Two articles on the PABI project have appeared in the popular press:

1. Newsweek, June 6 issue
2. Reader's Digest, August issue

Pdf copies of these stories are included as an appendix.

Mark Robert is modifying existing psychophysical testing software and programming new experiments for pitch ranking and comparisons of surface and penetrating electrodes, and for comparing pitch in PABI and acoustic hearing for PABI#3 who has residual hearing in contralateral ear. New experiments are being programmed to investigate the ability of PABI patients to integrate basic psychophysical percepts into phoneme classification. One potential issue identified in speech recognition is that patients have relatively normal psychophysical performance but poor speech identification. Studies will target the ability of listeners to combine perceptual information to achieve phoneme identification.

REFERENCES

R. L. Snyder, P. A. Leake, and G. T. Hradek, "Quantitative analysis of spiral ganglion projections to the cat cochlear nucleus," *J Comp Neurol*, vol. 379, pp. 133-49, 1997.

M.N. Semple and L.M. Aitkins. “ Representation of sound frequencies and laterality by units in the central nucleus of cat inferior colliculus”, J. Neurophysiology, vol. 42 pp. 1629-1639, 1979

D. B. McCreery, R. V. Shannon, J. K. Moore, and M. Chategee, "Accessing the tonotopic organization of the ventral cochlear nucleus by intranuclear microstimulation," *IEEE Transactions on Rehabilitation Engineering*, vol. 23, pp. 391-399, 1998.